


Effects of uteroplacental insufficiency on cardiac development in growth-restricted newborn rats

Hsiu-Chu Chou¹ and Chung-Ming Chen^{2,3} 

Original Article

Cite this article: Chou H-C and Chen C-M. (2023) Effects of uteroplacental insufficiency on cardiac development in growth-restricted newborn rats. *Journal of Developmental Origins of Health and Disease* **14**: 272–278. doi: [10.1017/S2040174422000575](https://doi.org/10.1017/S2040174422000575)

Received: 2 May 2022
Revised: 11 September 2022
Accepted: 15 September 2022
First published online: 14 October 2022

Keywords:

Uteroplacental insufficiency; fetal growth restriction; glycogen; collagen; pulmonary hypertension

Address for correspondence:

Chung-Ming Chen, Department of Pediatrics, Taipei Medical University Hospital, Taipei 110, Taiwan.
Email: cmchen@tmu.edu.tw

¹Department of Anatomy and Cell Biology, School of Medicine, College of Medicine, Taipei Medical University, Taipei, Taiwan; ²Department of Pediatrics, Taipei Medical University Hospital, Taipei, Taiwan and ³Department of Pediatrics, School of Medicine, College of Medicine, Taipei Medical University, Taipei, Taiwan

Abstract

Fetal growth restriction (FGR) is associated with reduced cardiac function in neonates. Uteroplacental insufficiency (UPI) is the most common cause of FGR. The mechanisms underlying these alterations remain unknown. We hypothesized that UPI would influence cardiac development in offspring rats. Through this study, we evaluated the effects of UPI during pregnancy on heart histology and pulmonary hypertension in growth-restricted newborn rats. On gestation Day 18, either UPI was induced through bilateral uterine vessel ligation (FGR group) or sham surgery (control group) was performed. The right middle lobe of the lung and the heart were harvested for histological and immunohistochemical evaluation on postnatal days 0 and 7. The FGR group exhibited significantly lower body weight, hypertrophy and degeneration of cardiomyocytes, increased intercellular spaces between the cardiomyocytes and collagen deposition, and decreased glycogen deposition and HNK-1 expression compared with the control group on postnatal days 0 and 7. These results suggest that neonates with FGR may have inadequate myocardial reserves, which may cause subsequent cardiovascular compromise in future life. Further studies are required to evaluate the hemodynamic changes in these growth-restricted neonates.

Introduction

Uteroplacental insufficiency (UPI) affects nearly 10% of human pregnancies and is the most common cause of fetal growth restriction (FGR).¹ It is characterized by decreased placental function and compromised nutrient and oxygen delivery to the fetus.² The situations leading to FGR are the illnesses intrinsic to the fetal-placental-maternal unit, fetal undernutrition, and intrauterine space constraints restricting the fetal growth. The most common cause of FGR are preeclampsia, diabetes, anemia, chronic lung or kidney diseases, poor nutrition, alcohol or drug use, cigarette smoking, multiple gestation, infections, and genetic disorders.³ Recent evidence proposes that being born with growth restriction is associated with reduced cardiac function and increased cardiovascular risk in infants, children, and adults.^{4–6} FGR neonates exhibited altered cardiac development and cardiac morphology and subclinical myocardial dysfunction.⁷ However, the mechanisms underlying these alterations remain unknown in neonates. FGR increases the risk of pulmonary hypertension in premature infants.^{8,9} Preclinical studies demonstrated that Sprague–Dawley rats born to undernourished mothers did not exhibit pulmonary hypertension at 6, 12, and 14 weeks.^{10–12} The short-term effects of FGR on pulmonary hypertension were largely unknown in neonates. FGR is caused by different factors such as decreased placental perfusion or maternal nutritional deficiencies in humans. In this study, we used the UPI model of FGR in rats, as it resembles human illness and is thus, widely used.¹³ We hypothesized that UPI would influence cardiac development in the offspring rats. Through this study, we aimed to evaluate the effects of UPI during pregnancy on heart histology and pulmonary hypertension in growth-restricted newborn rats.

Methods

Ethical approval

All procedures were approved by the Institutional Animal Care and Use Committee of Taipei Medical University and performed according to a protocol approved by the Association for Assessment and Accreditation of Laboratory Animal Care.

Animal model

Time-dated pregnant Sprague–Dawley rats were obtained from BioLASCO Taiwan Co., Ltd. (Yilan, Taiwan) and housed in clean specific pathogen-free rooms under a 12-h light-dark cycle

with ad libitum access to laboratory food and water. On day 18 of pregnancy, bilateral uterine artery ligation was performed to induce intrauterine growth retardation (FGR group), whereas the control group were subjected to a sham protocol.¹⁴ All rats were delivered naturally at term (22 days). Litters were separated from their mothers within 12 h of birth, pooled, and randomly redistributed to the newly delivered mothers. Rats were randomly selected for examination from each group, irrespective of sex, on postnatal days 0 and 7.

Tissue collection

Animals were deeply anesthetized with isoflurane and euthanized by cardiac puncture and exsanguination. The right middle lobe of the lung and the heart were harvested and fixed in 4% paraformaldehyde for 48 h. After being washed with phosphate-buffered saline (PBS), the heart was dissected into atria and ventricles followed by serial dehydration in increasing concentrations of ethanol and xylene infiltration before being embedded in paraffin. Serial 5- μ m-thick paraffin sections of the lungs and ventricles were cut serially using a microtome. The ventricle was sectioned from base to apex. Sample sections were subjected to histological evaluation and immunohistochemical processing.

Histological assessment and morphological analysis

After routine deparaffinization, the sections of the lung and the ventricle were stained with hematoxylin and eosin, periodic acid-Schiff (PAS), and Masson's trichrome, and examined by light microscopy to assess the lung and heart morphology. The heart section at 40 \times magnification and five randomly selected fields from each lung section at 400 \times magnification were captured using a digital camera and imported into a computerized image analysis system (Image-Pro Plus 6.0 for Windows, Media Cybernetics, Silver Spring, MD, USA) for morphological quantification. Right ventricular (RV) hypertrophy was assessed by measuring the ratio of the RV wall thickness (RVWT) to the left ventricular wall thickness (LVWT) and interventricular septum thickness (IVST) as follows: RV hypertrophy = RVWT/LVWT + IVST.¹⁵ The measurement of the LV relative wall thickness (RWT) was modified from the study by Hashem *et al.*¹⁶ Calculations were performed by dividing the sum of the IVST and posterior LV wall thickness (PLVWT) by the diameter of the left ventricle (DLV). Each wall thickness was measured from the middle of the longitudinal length of its wall, and the transverse length (wall thickness) was in the range between the free edges on both sides (Fig. 1a). The medial wall thickness (MWT) of the pulmonary arteries was measured in vessels with an external diameter of 20–65 μ m, and those having external diameters measured at two perpendicular planes within 33% of each other were included in the counts. In total, 20 vessels were measured in each animal. The percent medial thickness of an individual vessel was calculated using the following formula: medial thickness (MT) \times 2 \times 100/external diameter (Fig. 1b).¹⁷ The thickness of ventricular walls and interventricular septum of the heart, and the external diameter and wall thickness of the lung were measured using Image-Pro Plus (Media Cybernetics, Silver Spring, MD, USA).

Immunohistochemistry

Immunostaining was performed on the ventricle sections using the streptavidin-peroxidase technique. After routine deparaffinization, heat-induced epitope retrieval was performed by immersing the slides in 0.01 M sodium citrate buffer (pH 6.0). For block endogenous peroxidase activity and nonspecific antibody binding,

the sections were first pre-incubated for 1 h at room temperature in 0.1 M PBS containing 10% normal goat serum and 0.3% H₂O₂ before being incubated for 20 h at 4°C with mouse IgM monoclonal anti-human Leu-7 (HNK-1) antibody (1:80 diluted; Becton-Dickinson Immunocytometry Systems, Mountain View, CA, USA) as the primary antibody. The sections were then treated for 1 h at 37°C with biotinylated goat anti-mouse IgG (1:200, Jackson ImmunoResearch Laboratories Inc., West Grove, PA, USA). Sections were treated with reagents from an avidin-biotin complex kit (Vector Laboratories, Inc., Burlingame, CA, USA), and brown reaction products were visualized using a diaminobenzidine substrate kit (Vector Laboratories) according to the manufacturer's recommendations. All immunostained sections were viewed and photographed using a Nikon Eclipse E600 Microscope (Nikon, Tokyo, Japan). Five randomly selected fields from each section at 400 \times magnification were captured using a digital camera and imported into a computerized image analysis system (Image-Pro Plus 6.0 for Windows, Media Cybernetics).

Statistical analysis

All data are presented as mean \pm standard deviation with SPSS 23.0 (SPSS Inc., Chicago, IL, USA) used for statistical analyses. Differences between control and FGR groups on each postnatal day were analyzed by Student's *t*-test. The differences were considered statistically significant at $p < 0.05$.

Results

Uteroplacental insufficiency reduced body weight in growth-restricted newborn rats

Four sham-operated dams delivered 39 control rats and four UPI-induced dams delivered 26 FGR rats. On postnatal days 0 and 7, we retrieved 12 and 8 pups from the sham-operated and UPI-induced dams, respectively. The remaining dams and pups after postnatal day 7 were not used. Compared with control rats, rats with FGR exhibited significantly lower body weights on postnatal days 0 and 7 and significantly a higher heart to body weight ratio on postnatal day 0 (Table 1). The heart weights were comparable between the control and FGR groups on postnatal days 0 and 7.

Effects of uteroplacental insufficiency on ventricular histology

Significant hypertrophy and degeneration of ventricular cardiomyocytes were observed near the subendothelial layer in rat hearts on postnatal days 0 and 7 (Fig. 2). Cells were swollen, and organelles and nuclei were integrated to form enlarged foam cells that clumped together to form clusters within the myocardium beneath the subendothelial layer. Masson's trichrome staining revealed that the collagen fibers in the FGR groups were deposited between cardiomyocytes (Fig. 3). However, in the control group, the results of Masson's trichrome staining were not as clear as in the FGR group, possibly owing to an insufficient number of collagen fibers in the extracellular space. In this scenario, cardiomyocytes in the FGR group had a larger extracellular space than did those in the control group. The concentration of glycogen in cardiomyocytes was detected by PAS method. PAS-positive staining was observed in many cardiomyocytes in the ventricular myocardium of control rats as pink purple in the cytoplasm of cardiomyocytes (Fig. 4), whereas fewer PAS-positively stained cardiomyocytes were observed in the ventricular myocardium in the FGR group.

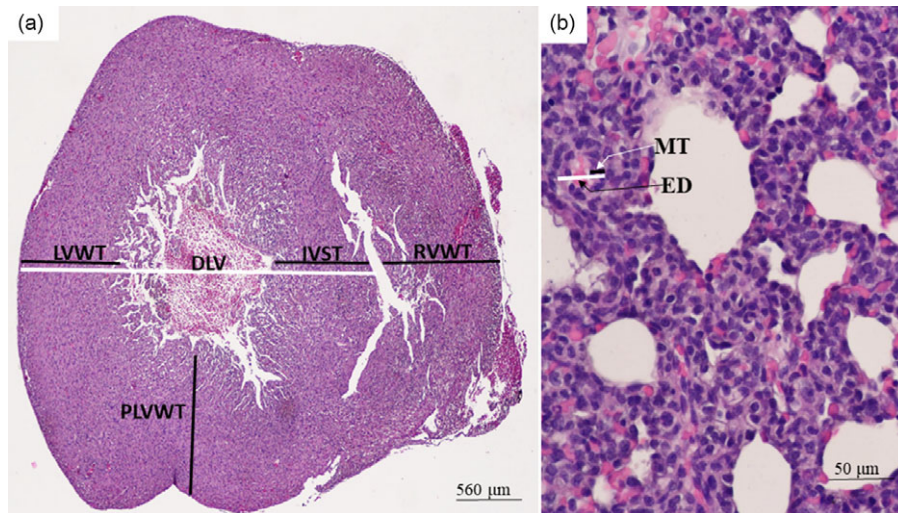


Fig. 1. Representative histological images of hematoxylin and eosin-stained heart and lung tissue sections. (a) Whole-heart cross-sectional dissection was performed to obtain transverse sections of the ventricles for morphometric analysis. (b) Photograph of lung section for morphometric analysis of medial wall thickness. RVWT: right ventricle wall thickness, LVWT: left ventricle wall thickness, IVST: interventricular septum thickness, PLVWT: posterior left ventricle wall thickness, DLV: diameter of the left ventricle, MT: medial thickness of vessel wall, ED: external diameter.

Table 1. Body and heart weights and heart:body weight ratios in control and FGR rats on postnatal days 0 and 7

Group	n	Body weight (g)	Heart weight (g)	Heart:body weight (%)
Postnatal day 0				
Control	12	6.40 ± 0.56	0.042 ± 0.005	0.66 ± 0.10
FGR	8	5.38 ± 0.88*	0.043 ± 0.007	0.83 ± 0.21*
Postnatal day 7				
Control	12	16.90 ± 1.39	0.113 ± 0.012	0.67 ± 0.10
FGR	8	14.50 ± 0.55*	0.106 ± 0.018	0.73 ± 0.14

Values are presented as means ± SD.

* $p < 0.05$ vs. control group at each postnatal age.

FGR: fetal growth restriction.

Uteroplacental insufficiency did not change ventricular morphometry in growth-restricted newborn rats

The LV RWT was assessed using the following equation: $RWT = IVST + PLVWT/DLV$. RV hypertrophy was assessed using the following equation: $RVWT/LVWT + IVST$. The indicators of LV hypertrophy (RWT) and RV hypertrophy ($RVWT/LVWT + IVST$) were compatible between control and FGR rats on postnatal days 0 and 7 (Fig. 5).

Effects of uteroplacental insufficiency on MWT

The MWT of lung vessels provides an index for evaluating pulmonary hypertension. We estimated arterial remodeling by measuring the MWT of the small pulmonary arteries (external diameter of 20–65 μm). No significant difference was observed in the percentage of pulmonary vessel lining thickening between control and FGR rats on postnatal days 0 and 7 (Fig. 6).

Uteroplacental insufficiency reduced HNK-1 expression in growth-restricted newborn rats

HNK-1 was immunoassayed to delineate the conducting tissues. HNK-1 immunoreactivity was detected in the subendocardium, the region between the myocardium and the endocardium, of

the left and right ventricles, and more HNK-1 immunoreactivity was detected on postnatal day 7 (Fig. 7a). Less HNK-1 immunoreactivity was detected in the FGR group than in the control group on postnatal days 0 and 7. FGR rats had significantly lower optical density of HNK-1 compared with control rats on postnatal days 0 and 7 (Fig. 7b).

Discussion

Our *in vivo* model demonstrated that UPI through bilateral uterine ligation reduced body weight and altered ventricular histology, as evidenced by hypertrophy and degeneration of cardiomyocytes, increased intercellular spaces between the cardiomyocytes and collagen deposition, and decreased glycogen deposition and HNK-1 expression on postnatal days 0 and 7. These findings indicate that UPI during pregnancy induced FGR and ventricle histological alteration and did not induce pulmonary hypertension in the immediate neonatal period. These results suggest that neonates with FGR may have inadequate myocardial reserves at birth, which may influence subsequent cardiovascular compromise in future life.^{4–6}

Takahashi *et al.* reported that four extremely-low-birthweight infants with severe FGR died 5–10 days after birth owing to heart failure, and autopsy findings revealed hypoplasia of myocardial fibers and decreased glycogen levels.¹⁸ The researchers suggested that the hearts of these infants failed to adapt to postnatal hemodynamic changes because of inadequate myocardial function and inadequate glycogen reserves. Our results that FGR rats exhibited reduced glycogen in ventricles at birth support these clinical findings and suggest that infants who are small for gestational age need to be closely monitored for hemodynamic status. Tsirka *et al.* used a similar animal model of FGR in Sprague–Dawley rats and found no significant difference in the glycogen content between the hearts of control and FGR rats.¹⁹ This discrepancy may be attributable to the fact that they performed bilateral uterine ligation at a gestational age of 19 days and measured glycogen content on postnatal days 21 and 120.

The effects of FGR on the incidence of pulmonary hypertension differ in human and animal studies.^{8–12} In the current study, we evaluated pulmonary hypertension by measuring LV and RV hypertrophy and MWT in the lungs and found that rats with FGR did not exhibit increased pulmonary hypertension. These

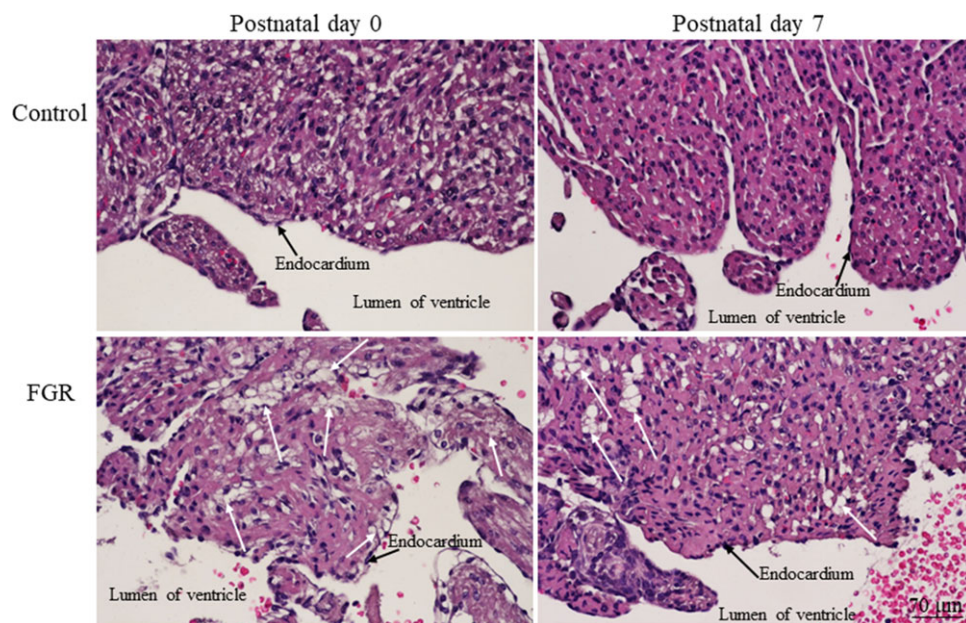


Fig. 2. Representative ventricular sections stained with hematoxylin and eosin. Significant hypertrophy and degeneration of ventricular cardiomyocytes were observed near the subendothelial layer on postnatal days 0 and 7 (white arrow).

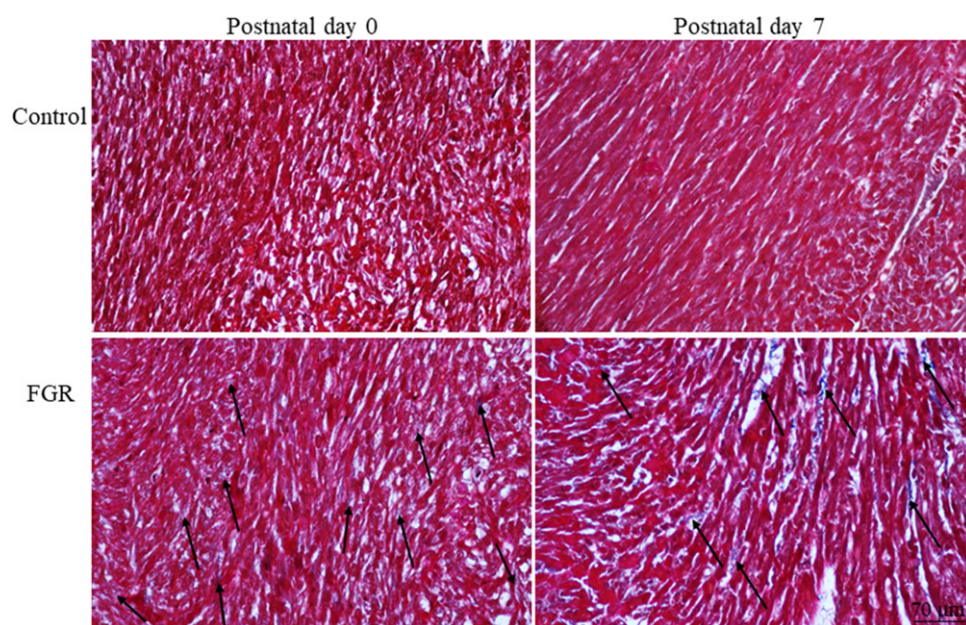


Fig. 3. Representative ventricular sections stained by Masson's trichrome. The collagen fibers were deposited between the cardiomyocytes. The FGR group exhibited more collagen deposition and larger extracellular space (black arrow) than did the control group on postnatal days 0 and 7.

results suggest that pulmonary hypertension was mostly due to postnatal events that influence cardiovascular adaptation during the transitional period in growth-restricted infants.²⁰

Term infants who are small for gestational age have reduced heart rate variability and heart rate reflex responses at 1 month of age compared with term infants who are an appropriate size for gestational age.²¹ FGR has been reported to be associated with prolonged time intervals between early ventricular inflow and atrial contraction.²² HNK-1 is an established marker of the cardiac conduction system development and is useful for the analysis of abnormal conduction system.²³ Therefore, we immunoassayed HNK-1 to evaluate the effect of FGR on cardiac conduction in rats. We found that FGR rats exhibited significantly less HNK-1 expression compared with control rats on postnatal days 0 and 7. These

findings might explain the reduced cardiac reflexes in growth-restricted infants.

Our study has several limitations. First, we did not measure hemodynamic parameters such as RV systolic pressure, cardiac index, total pulmonary resistance index, and systolic arterial pressure; however, a related study has revealed that hemodynamic parameters are comparable to histologic morphometry.²⁴ Second, we used the expression of these proteins in whole tissue sections for immunohistochemistry studies. Many studies have confirmed the correlation between immunohistochemistry and the tissue concentration of the antigen.²⁵ Third, we did not determine the sex of the offspring though the sex effects of FGR on cardiac development during immediate postnatal period were unknown. In maternal undernutrition, male

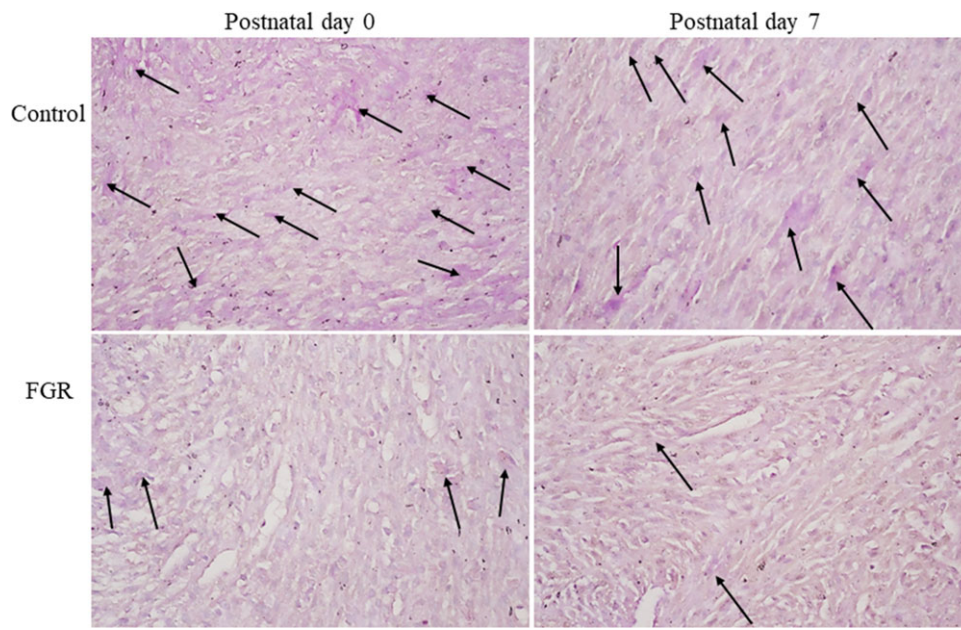


Fig. 4. Representative ventricular sections stained with periodic acid-Schiff stain. The glycogen was stained pink purple in the cytoplasm of cardiomyocytes (black arrow). The FGR group exhibited less glycogen than did the control group on postnatal days 0 and 7.

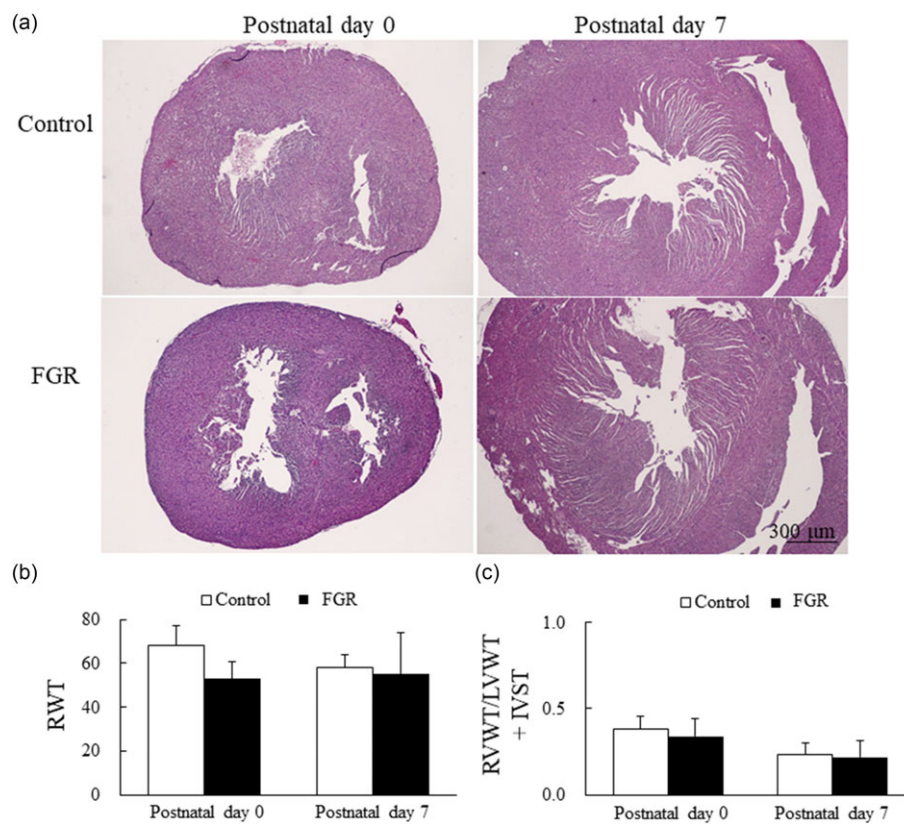


Fig. 5. (a) Representative images of whole-heart transverse cross section stained by hematoxylin and eosin, (b) indicators of left ventricular hypertrophy (RWT), and (c) indicators of right ventricular hypertrophy (RVWT/LVWT + IVST) in the control and FGR rats. The RWT and RVWT/LVWT + IVST were comparable between control and FGR rats on postnatal days 0 and 7. Data are expressed as mean \pm SD.

rat offspring exhibited larger heart weight/body weight ratio on postnatal day 21 and male fetal baboon showed left ventricular fibrosis inversely correlated with birth weight.^{26,27} Further studies are needed to determine the sex-specific differences in cardiac development of growth-restricted offspring. Despite these limitations, the results of the present study provide valuable data that demonstrate the mechanisms and potential harmful effects of UPI in growth-restricted neonates.

In conclusion, this study demonstrated that UPI, through bilateral uterine ligation, induced FGR and led to changes in ventricular histology but did not induce pulmonary hypertension in the immediate neonatal period. These results might partly explain the underlying mechanism of reduced cardiac function in infants with FGR and subsequent cardiovascular compromise in future life. Further studies are required to evaluate hemodynamic changes in these growth-restricted neonates.

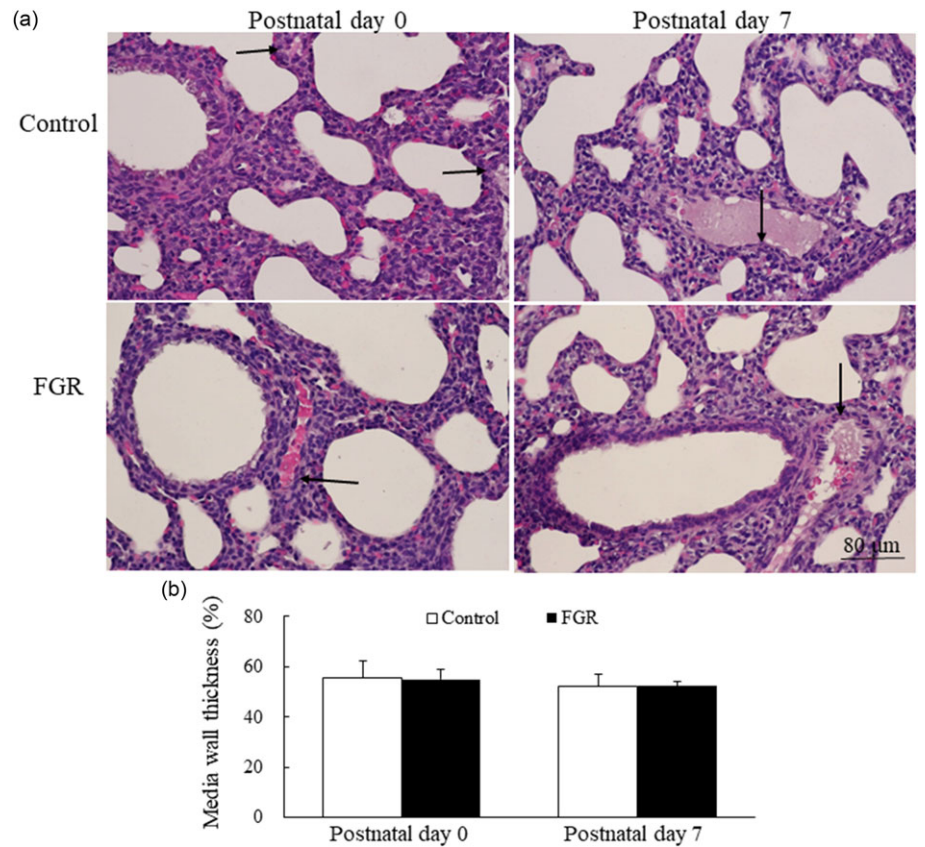


Fig. 6. (a) Representative lung sections stained with hematoxylin and eosin and (b) medial wall thickness (MWT) in control and FGR rats. The MWT was comparable between control and FGR rats on postnatal days 0 and 7. Black arrow indicates the tunica media of the artery.

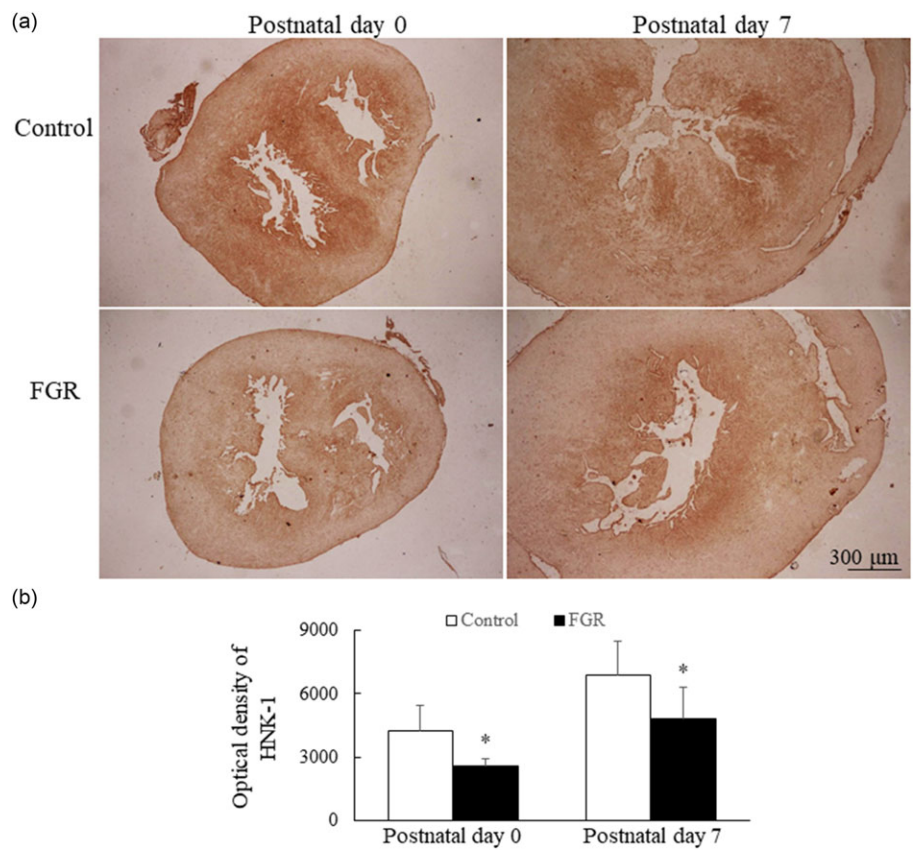


Fig. 7. (a) Representative photomicrographs and (b) optical density of HNK-1. Positive immunoreactivity is indicated by brown staining. HNK-1 immunoreactivity was detected in the subendocardium, and higher HNK-1 immunoreactivity was detected on postnatal day 7. FGR rats displayed significantly lower optical density of HNK-1 compared with control rats on postnatal days 0 and 7. Data are expressed as mean ± SD. * $p < 0.01$ vs. control group on each postnatal day.

Acknowledgments. None.

Financial support. This study was supported by a grant from Taipei Medical University Hospital (111TMUH-MOST-15), Taipei, Taiwan.

Conflicts of interest. None.

Ethical standards. The authors assert that all procedures contributing to this work comply with the ethical standards of the Association for Assessment and Accreditation of Laboratory Animal Care and have been approved by the Institutional Animal Care and Use Committee of Taipei Medical University.

References

- Henriksen T, Clausen T. The fetal origins hypothesis: placental insufficiency and inheritance versus maternal malnutrition in well-nourished populations. *Acta Obstet Gynecol Scand.* 2002; 81(2), 112–114.
- Wu G, Bazer FW, Wallace JM, Spencer TE. Board-invited review: intrauterine growth retardation: implications for the animal sciences. *J Anim Sci.* 2006; 84(9), 2316–2337.
- Blue NR, Page JM, Silver RM. Recurrence risk of fetal growth restriction: management of subsequent pregnancies. *Obstet Gynecol Clin North Am.* 2021; 48(2), 419–436.
- Cohen E, Wong FY, Horne RS, Yiallourou SR. Intrauterine growth restriction: impact on cardiovascular development and function throughout infancy. *Pediatr Res.* 2016; 79(6), 821–830.
- Nordman H, Jääskeläinen J, Voutilainen R. Birth size as a determinant of cardiometabolic risk factors in children. *Horm Res Paediatr.* 2020; 93(3), 144–153.
- Crispi F, Rodríguez-López M, Bernardino G, et al. Exercise capacity in young adults born small for gestational age. *JAMA Cardiol.* 2021; 6(11), 1308–1316.
- Zaharie GC, Hasmasanu M, Blaga L, Matyas M, Muresan D, Bolboacă SD. Cardiac left heart morphology and function in newborns with intrauterine growth restriction: relevance for long-term assessment. *Med Ultrason.* 2019; 21(1), 62–68.
- Check J, Gotteiner N, Liu X, et al. Fetal growth restriction and pulmonary hypertension in premature infants with bronchopulmonary dysplasia. *J Perinatol.* 2013; 33(7), 553–557.
- Vyas-Read S, Kanaan U, Shankar P, et al. Early characteristics of infants with pulmonary hypertension in a referral neonatal intensive care unit. *BMC Pediatr.* 2017; 17(1), 163.
- Lv Y, Tang LL, Wei JK, et al. Decreased Kv1.5 expression in intrauterine growth retardation rats with exaggerated pulmonary hypertension. *Am J Physiol Lung Cell Mol Physiol.* 2013; 305(11), L856–L865.
- Xu XF, Lv Y, Gu WZ, et al. Epigenetics of hypoxic pulmonary arterial hypertension following intrauterine growth retardation rat: epigenetics in PAH following IUGR. *Respir Res.* 2013; 14(1), 20.
- Fu LC, Lv Y, Zhong Y, He Q, Liu X, Du LZ. Tyrosine phosphorylation of Kv1.5 is upregulated in intrauterine growth retardation rats with exaggerated pulmonary hypertension. *Braz J Med Biol Res.* 2017; 50(11), e6237.
- Janot M, Cortes-Dubly ML, Rodriguez S, Huynh-Do U. Bilateral uterine vessel ligation as a model of intrauterine growth restriction in mice. *Reprod Biol Endocrinol.* 2014; 12, 62.
- Huang LT, Chou HC, Lin CM, Chen CM. Uteroplacental insufficiency alters retinoid pathway and lung development in the newborn rats. *Pediatr Neonatol.* 2016; 57(6), 508–514.
- de Visser YP, Walther FJ, Laghmani EH, Boersma H, Van der Laarse A, Wagenaar GT. Sildenafil attenuates pulmonary inflammation and fibrin deposition, mortality and right ventricular hypertrophy in neonatal hyperoxic lung injury. *Respir Res.* 2009; 10(1), 30.
- Hashem MS, Kalashyan H, Choy J, et al. Left ventricular relative wall thickness versus left ventricular mass index in non-cardioembolic stroke patients. *Medicine.* 2015; 94(20), e872.
- Masood A, Yi M, Lau M, et al. Therapeutic effects of hypercapnia on chronic lung injury and vascular remodeling in neonatal rats. *Am J Physiol Lung Cell Mol Physiol.* 2009; 297(5), L920–L930.
- Takahashi N, Nishida H, Arai T, Kaneda Y. Abnormal cardiac histology in severe intrauterine growth retardation infants. *Acta Paediatr Jpn.* 1995; 37(3), 341–346.
- Tsirka AE, Gruetzmacher EM, Kelley DE, Ritov VH, Devaskar SU, Lane RH. Myocardial gene expression of glucose transporter 1 and glucose transporter 4 in response to uteroplacental insufficiency in the rat. *J Endocrinol.* 2001; 169(2), 373–380.
- Abbas G, Shah S, Hanif M, et al. The frequency of pulmonary hypertension in newborn with intrauterine growth restriction. *Sci Rep.* 2020; 10(1), 8064.
- Galland BC, Taylor BJ, Bolton DP, Sayers RM. Heart rate variability and cardiac reflexes in small for gestational age infants. *J Appl Physiol.* 2006; 100(3), 933–939.
- Kurihara Y, Tachibana D, Yokoi N, et al. Time-interval changes of cardiac cycles in fetal growth restriction. *Eur J Obstet Gynecol Reprod Biol.* 2016; 203, 152–155.
- Kise K, Nakagawa M, Okamoto N, et al. Teratogenic effects of bis-diamine on the developing cardiac conduction system. *Birth Defects Res A Clin Mol Teratol.* 2005; 73(8), 547–554.
- Hessel MH, Steendijk P, den Adel B, Schutte CI, van der Laarse A. Characterization of right ventricular function after monocrotaline-induced pulmonary hypertension in the intact rat. *Am J Physiol Heart Circ Physiol.* 2006; 291(5), H2424–H2430.
- Matos LL, Truffelli DC, de Matos MG, da Silva Pinhal MA. Immunohistochemistry as an important tool in biomarkers detection and clinical practice. *Biomark Insights.* 2010; 5(5), 9–20.
- Rodríguez-Rodríguez P, López de Pablo AL, García-Prieto CF, et al. Long term effects of fetal undernutrition on rat heart. Role of hypertension and oxidative stress. *PLoS One.* 2017; 12(2), e0171544.
- Muralimanoharan S, Li C, Nakayasu ES, et al. Sexual dimorphism in the fetal cardiac response to maternal nutrient restriction. *J Mol Cell Cardiol.* 2017; 108, 181–193.